Deformation Potentials of the Indirect and Direct Absorption Edges of AlSb†

LUCIEN D. LAUDE,* MANUEL CARDONA, AND FRED H. POLLAK
Physics Department, Brown University, Providence, Rhode Island 02912
(Received 7 July 1969)

The splittings and shifts of the phonon-aided indirect exciton edge ($\Gamma_{15} \rightarrow X_1$) of AlSb produced by uniaxial stresses along [001], [111], and [110] have been determined. These measurements were performed at 77°K, using the wavelength-modulation technique. TO-phonon-assisted transitions, not reported previously, have been identified in the spectrum of the stressed materials; they yield a TO-phonon energy at X of 42±3 meV. These measurements have also yielded the shear deformation potentials of the Γ_{15} valence band ($b=-1.35\pm0.1$ eV and $d=-4.3\pm0.4$ eV) and the X_1 conduction band ($\varepsilon_2=+5.4\pm0.3$ eV). The hydrostatic deformation potential of the indirect edge was found to be $a_i=+2.2\pm0.2$ eV. Electroreflectance measurements at room temperature of the direct edge ($\Gamma_{15} \rightarrow \Gamma_{1c}$) of this material under uniaxial compression along the [110] direction have also been performed. The stress-induced splitting of the Γ_{15} band observed in these measurements agrees with that obtained from the indirect exciton. The hydrostatic coefficient of the direct edge was found to be -5.9 ± 1.2 eV.

I. INTRODUCTION

THE III-V semiconductors of small band gap (e.g., InSb, InAs, etc.) are known to have a direct fundamental edge at $\mathbf{k}=0$.[1] The large-band-gap materials (BP,[2] GaP,[1] etc.) have an indirect fundamental edge which usually corresponds to transitions between the Γ_{15} valence-band maximum and conduction-band minima along [100], at or very close to the edge of the Brillouin zone (X).[1] AlSb, with a moderately large absorption edge (1.69 eV at 77°K), is known to be an indirect-edge material.[3,4] The corresponding conduction-band minima occur along [100].[5,6] The exact positions of these minima are not known, but they should occur close to X if not exactly at X. The lowest direct gap of this material ($\Gamma_{15} \rightarrow \Gamma_{1c}$) occurs at 2.2 eV.[7,8]

The band structure of AlSb, calculated by the $\mathbf{k}\cdot\mathbf{p}$ method with inclusion of spin-orbit interaction,[9] is shown in Fig. 1. The fact that in this figure the conduction-band minimum does not occur exactly at X is not to be taken as decisive, since a small modification of the parameters of the calculation suffices to bring this minimum to X. The X_1–X_3 labeling of the conduction band states at X is arbitrary since it is determined by the choice of origin of coordinates. For GaP it is well established that the labeling of Fig. 1 corresponds to taking the phosphorus atom as origin.[10] The lowest conduction band X_1 yields a charge distribution concentrated mainly around the group-V atom. As we shall see in Sec. III, our experiments suggest that the charge distribution of the lowest conduction-band state of AlSb is concentrated mainly around the group-III atom. A number of gaps (E_1, $E_1+\Delta_1$, E_2) observed in the reflectivity of AlSb[11] are indicated by arrows. In addition, the spin-orbit splitting of the Γ_{15} valence band has been observed in the absorption spectrum of p-type AlSb.[12]

Modulation techniques have been very helpful in elucidating the optical properties of AlSb. Electroreflectance[7] and thermoreflectance[13] measurements have yielded accurate values of the gaps of Fig. 1, and wavelength-modulated absorption[3] has yielded the value of the indirect edge and the energies of phonons (LO, LA, TA) near X. In this work we have used the wavelength-modulation technique[3,14] to study the effect of uniaxial stress on the indirect edge of AlSb (at 77°K). We have also used the electroreflectance technique (at room temperature)[7] to study the effect of uniaxial stress on the direct edge of this material.

It is known[15] that a uniaxial stress splits the Γ_{15} valence-band state of a zinc-blende-type material. The splitting due to the pure shear component of the stress can be completely described, for an arbitrary stress direction, by two deformation potentials (b and d).[15] A uniaxial stress may also split the equivalent X conduction-band minima. This splitting is completely

† Supported by the National Science Foundation, the Advanced Research Projects Agency, and the U. S. Army Research Office (Durham).

* NASA Postdoctoral International University Fellow, sponsored by the European Space Research Organization.

[1] See, for example, O. Madelung, *Physics of III-V Compounds* (John Wiley & Sons, Inc., New York, 1964).

[2] R. J. Archer, R. Y. Koyama, E. E. Loebner, and R. C. Lucas, Phys. Rev. Letters **12**, 538 (1964).

[3] J. E. Rowe, K. L. Shaklee, and M. Cardona, Solid State Commun. **7**, 441 (1969).

[4] R. F. Blunt, H. P. R. Frederikse, J. H. Becker, and W. R. Hosler, Phys. Rev. **96**, 578 (1954).

[5] A. L. Edwards and H. G. Drickamer, Phys. Rev. **122**, 1149 (1961).

[6] K. M. Ghanekar and R. J. Sladek, Phys. Rev. **146**, 505 (1966).

[7] M. Cardona, F. H. Pollak, and K. L. Shaklee, Phys. Rev. Letters **16**, 644 (1966); M. Cardona, K. L. Shaklee, and F. H. Pollak, Phys. Rev. **154**, 696 (1967).

[8] C. A. Mead and W. G. Spitzer, Phys. Rev. Letters **11**, 358 (1963).

[9] F. H. Pollak, C. W. Higginbotham, and M. Cardona, J. Phys. Soc. Japan Suppl. **21**, 20 (1966).

[10] T. N. Morgan, Phys. Rev. Letters **21**, 819 (1968).

[11] T. Fischer, Phys. Rev. **139**, A1228 (1965).

[12] R. Braunstein, Bull. Am. Phys. Soc. **4**, 133 (1959).

[13] E. Matataqui, A. G. Thompson, and M. Cardona, Phys. Rev. **176**, 950 (1968).

[14] I. Balslev, Phys. Rev. **143**, 636 (1966).

[15] G. E. Picus and G. L. Bir, Fiz. Tverd. Tela. **1**, 154 (1959) [English transl.: Soviet Phys.—Solid State **1**, 136 (1959)].

described with one deformation potential $\mathcal{E}_2$.[16] The indirect edge of stressed AlSb should show these splittings (see Fig. 2) plus a shift due to the hydrostatic component of the stress (deformation potential a_i). The direct edge should show the same valence-band splittings plus a hydrostatic shift described by a deformation potential a_d. The experimental study of these splittings reported here leads to the determination of all these deformation potentials. The selection rules for the various transitions observed experimentally are considered and shown to be in qualitative agreement with the experimental observations. Wavelength-modulated absorption experiments under uniaxial stress have been reported by Balslev for the indirect edge of Ge, Si,[14] and GaP.[17] Electroreflectance measurement under stress (piezo-electroreflectance) of the direct edge of Ge and GaAs have been reported by Pollak and Cardona.[18]

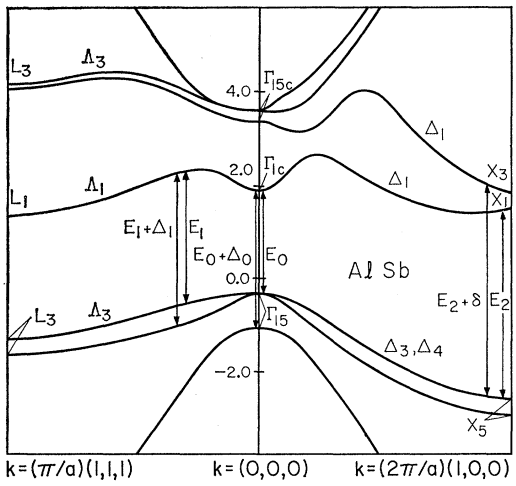

FIG. 1. Band structure of AlSb, as obtained by the $\mathbf{k}\cdot\mathbf{p}$ method (Ref. 9), in the [100] and [111] directions.

II. EXPERIMENT

The AlSb used for these experiments was obtained from Bell and Howell Inc.[19] The samples were x-ray oriented to $\pm 1°$ and cut into parallelepipeds of approximate dimensions $15\times 1.5\times 1.5$ mm, with the length along either the [001], [111], or [110] direction. They were mechanically polished and etched in a solution of Br in methanol. They were then coated with a solution of Lucite in ethylene dichloride so as to slow down tarnishing in air (AlSb is known to by hygroscopic). When not in use, the samples were kept in a desiccator. After several hours of exposure to room air, the transmission of the samples, even when coated, was found to decrease markedly, especially in the vicinity of the fundamental edge. The samples used for the wavelength-modulation studies of the indirect edge were p type and had a carrier density of 9×10^{16} cm^{-3}. Those used for the electroreflectance work were n type (tellurium doped) with $n=2\times 10^{18}$ cm^{-3}: The electroreflectance signals obtained with the more lightly doped p-type samples were considerably weaker.

The experimental technique used for the wavelength-modulation experiment has been described elsewhere.[20] The wavelength region of interest for the study of indirect excitons in AlSb was narrow enough and the exciton structure sharp enough to make the use of a double-beam system[20] unnecessary with the proper choice of grating and detector. We used a 600-lines/mm grating and a Dumont S-1 response photomultiplier. The light source was a Sylvania 600-W quartz-iodine lamp. The modulation unit was a silica plate vibrating at 23 Hz placed inside the monochromator in front of the entrance slit.

Electroreflectance measurements were performed at room temperature only, using as an electrolyte methanol with a few drops of HCl. With this nonaqueous electrolyte, the sample surface was found to be stable over the period of several hours required for the stress measurements. The stress was applied with the stressing apparatus described elsewhere.[18]

III. SYMMETRY CONSIDERATIONS AND EXPERIMENTAL RESULTS: INDIRECT EDGE

As mentioned in Sec. I, the fundamental edge of AlSb is indirect: Photon absorption is accompanied by

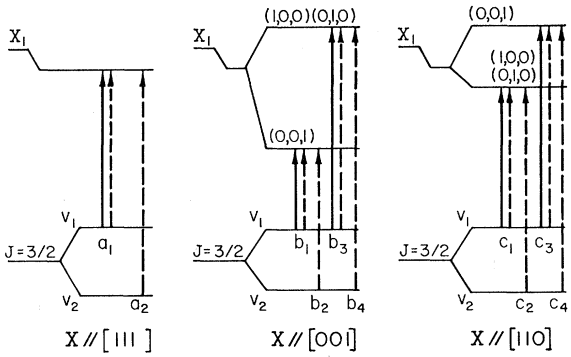

FIG. 2. Schematic representation of the stress-induced splittings and shifts of the Γ_{15} valence bands and X_1 conduction bands for compressive stress along the [111], [001], or [110] direction. The allowed transitions are given for the electric field vector of the incident light, **E**, parallel (solid lines) and perpendicular (dashed lines) to the stress direction. Not shown is the weak transition originating from the v_2 valence band for the case of stress along [110] and $\mathbf{E}\|X$ (see Table I).

[16] H. Brooks, in *Advances in Electronics and Electron Physics*, edited by L. Marton (Academic Press Inc., New York, 1955), Vol. 7, p. 85. We have used script $\mathcal{E}$'s to indicate the deformation potentials in order to avoid confusion with the symbol used for energy.

[17] I. Balslev, J. Phys. Soc. Japan Suppl. **21**, 101 (1966).

[18] F. H. Pollak and M. Cardona, Phys. Rev. **172**, 816 (1968).

[19] Bell and Howell, Inc., Pasadena, Calif.

[20] K. L. Shaklee, J. E. Rowe, and M. Cardona, Phys. Rev. **174**, 828 (1968); K. L. Shaklee, Thesis, Brown University, 1968 (unpublished).

TABLE I. Theoretical expressions for the relative intensities of the LA-phonon-assisted indirect exciton transitions, with Γ_{1c} as the intermediate state, for stress along [111], [001], or [110] with light polarized parallel and perpendicular to the stress axis.

		$\mathbf{E}\parallel X$	$\mathbf{E}\perp X$
$X\parallel[111]$	$I(a_1)$	$\frac{2}{3}(1+\alpha_1)$	$\frac{1}{6}(1-2\alpha_1)$
	$I(a_2)$	0	$\frac{1}{2}$
$X\parallel[001]$	$I(b_1)=\frac{1}{2}I(b_3)$	$\frac{2}{3}(1+\alpha_0)$	$\frac{1}{6}(1-2\alpha_0)$
	$I(b_2)=\frac{1}{2}I(b_4)$	0	$\frac{1}{2}$
$X\parallel[110]$	$I(c_3)=\frac{1}{2}I(c_1)$	$\frac{2}{3}(1+\alpha_2)$	$\frac{1}{6}(1-2\alpha_2)$
	$I(c_4)=\frac{1}{2}I(c_2)$	$\frac{1}{2}\epsilon^2$	$\frac{1}{2}(1-\epsilon)$

$$\epsilon=(\delta E_{001}-\delta E_{111})/(\delta E_{001}+3\delta E_{111})$$
$$\alpha_1=\delta E_{111}/\Delta_0$$
$$\alpha_0=\delta E_{001}/\Delta_0$$
$$\alpha_2=(\delta E_{111}/\Delta_0)[1+(\delta E_{001}-\delta E_{111})/4\delta E_{111}]$$

the absorption or emission of a phonon of $\mathbf{k}$ vector along equivalent $\langle 001\rangle$ directions, near X. For the purposes of this paper, it is reasonable to assume that the conduction-band minima occur at X. Of the possible intermediate states for the indirect transitions, the Γ_{1c} conduction band (Fig. 1) should give by far the smallest energy denominator and, hence, it is reasonable to assume that it gives the largest contribution to the indirect transition probability. Only phonons at X which are invariant under the operations of the group of the $\mathbf{k}$ vector at X are able to produce $\Gamma_{1c}\rightarrow X_1$ transitions; these are either the LA or the LO phonons depending on the choice of origin imposed by the X_1 labeling of the lowest conduction-band minimum.[10] The LA phonon corresponds to the vibration of the heavier atom and, thus, has X_1 symmetry if the origin of coordinates is at the site of the lighter atom. We find experimentally that the strongest indirect transitions are LA-phonon-aided although weak LO-, TO-, and TA-assisted transitions are also observed. This implies that if the Γ_{1c} intermediate state is indeed dominant, the electron density at the lowest conduction-band state must be concentrated around the group-III atom (Al). This conclusion is in contrast to that obtained for GaP [10]: In this material the LA-phonon-aided transitions are also the strongest and, thus, the electron density at X must be concentrated around the lighter group-V atom. We shall base our determination of deformation potentials on the behavior of the strong LA-emission lines (LA_e). Weak phonon-absorption lines are also observable for the four phonons at X.

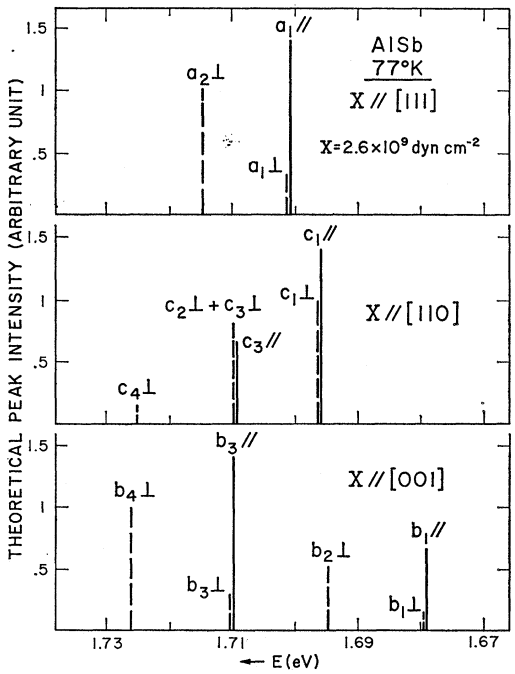

FIG. 3. Theoretical peak intensities of indirect transitions via Γ_{1c} for a stress of 2.6×10^9 dyn cm^{-2} along [111], [110], or [001].

A. Stress along [111]

For [111] stress, no intervalley splitting of the [001] conduction bands takes place. The splitting of the indirect exciton edge is expected to be due to the splitting of the top Γ_{15} valence band into the $(\frac{3}{2},\frac{3}{2})$ and the $(\frac{3}{2},\frac{1}{2})$ bands (v_2 and v_1, respectively, in Fig. 2). The energies of the split edges are given by[18]

$$\begin{aligned}\Delta(E_x-E_{v_2}\pm E_{\rm phon})&=\delta E_H+\tfrac{1}{2}\delta E_{111},\\ \Delta(E_x-E_{v_1}\pm E_{\rm phon})&=\delta E_H-\tfrac{1}{2}\delta E_{111}-\tfrac{1}{2}(\delta E_{111})^2/\Delta_0,\end{aligned}\tag{1}$$

to second order in the stress. Δ_0 is the spin-orbit splitting of the valence band. The linear hydrostatic and shear shifts δE_H and δE_{111} are, in terms of the corresponding deformation potentials a_i and d,

$$\begin{aligned}\delta E_H&=a_i(S_{11}+2S_{12})X,\\ \delta E_{111}&=(d/\sqrt{3})S_{44}X,\end{aligned}\tag{2}$$

where S_{11}, S_{12}, and S_{44} are the elastic compliance constants and X is the applied stress. Values of these

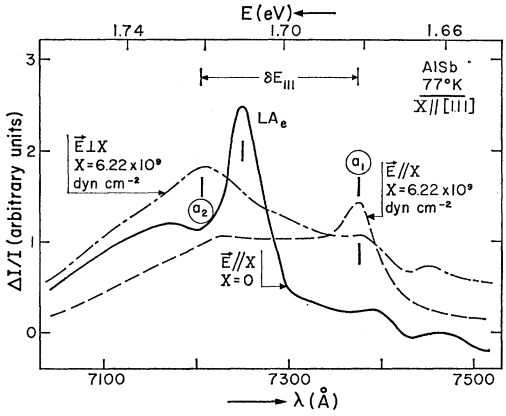

FIG. 4. Derivative transmission spectra for zero stress and for a stress of 6.22×10^9 dyn cm^{-2} applied along [111] with light polarized parallel and perpendicular to the stress axis.

TABLE II. Deformation potentials obtained in paper for AlSb.

Stress direction	d (eV)	$\delta E_{111}/X=(d/\sqrt{3})S_{44}$ (10^{-12} eV cm^2 dyn^{-1})	b (eV)	$\delta E_{001}/X=2b(S_{11}-S_{12})$ (10^{-12} eV cm^2 dyn^{-1})	$\delta E_{110}/X=\frac{1}{4}[d\sqrt{3}S_{44}+2b(S_{11}-S_{12})]$ (10^{-12} eV cm^2 dyn^{-1}) 77°K	295°K	a_i (eV)	a_d (eV)	ε_2 (eV)
[111]	−4.3 ±0.4	5.9±0.6					+2.2 ±0.2		
[001]			−1.35 ±0.1	5.8±0.6			+1.8 ±0.9		+5.4 ±0.3
[110]					5.5±0.8		+2.7 ±1.3		+5.1 ±0.7
[110][a]						6.4±1.3		−5.9 ±1.2	

[a] Obtained from room-temperature electroreflectance measurements.

compliance constants are not available at 77°K. However, from the existing data[1] for AlSb at room temperature and the previously reported variation of the elastic compliance constants of GaAs between 77°K and room temperature, we obtained the following values for AlSb at 77°K:

$$S_{11}=1.634\times10^{-12}\ \text{dyn}^{-1}\ \text{cm}^2,$$
$$S_{12}=-0.552\times10^{-12}\ \text{dyn}^{-1}\ \text{cm}^2,$$
$$S_{44}=2.38\times10^{-12}\ \text{dyn}^{-1}\ \text{cm}^2.$$

The room-temperature values of these constants are

$$S_{11}=1.661\times10^{-12}\ \text{dyn}^{-1}\ \text{cm}^2,$$
$$S_{12}=-0.549\times10^{-12}\ \text{dyn}^{-1}\ \text{cm}^2,$$
$$S_{44}=2.410\times10^{-12}\ \text{dyn}^{-1}\ \text{cm}^2.$$

We assume throughout this paper that the change of the exciton-binding energy with stress is negligible.[14]

The phonon-induced transitions between Γ_{1c} and X_1 are isotropic and, hence, the selection rules for the transition probability reflect exactly those for transitions between the split initial states (v_1,v_2) and the intermediate state Γ_{1c}. This would not be true for other intermediate states such as Γ_{15c}.[21] The intensities of the LA-assisted transitions via Γ_{1c} for both normal modes of polarization are given in Table I to first order in the ratio $\alpha_1=\delta E_{111}/\Delta_0$. The intensities of these lines are represented schematically in Fig. 3 for $\alpha_1\ll1$. If α_1 is not negligible, a change in the intensity of the a_1 lines linear with stress results. This change is produced by the coupling of the v_1 valence band to the lower spin-orbit split component of the Γ_{15} multiplet. This coupling is also responsible for the nonlinear shift of the a_1 line with stress shown in Eq. (1). Figure 4 shows the unstressed LA-phonon emission peak (LA_e) and the effect of a [111] compression of 6.22×10^9 dyn cm^{-2} for the electric field vector of the incident light (**E**) parallel and perpendicular to the stress. The hydrostatic shift in the average position of the peaks observed for both polarizations appears clearly. The shift with stress of the various phonon-aided transitions observed is shown in Fig. 5. While the LA_e peaks can be followed easily as a function of stress, the weaker additional peaks are

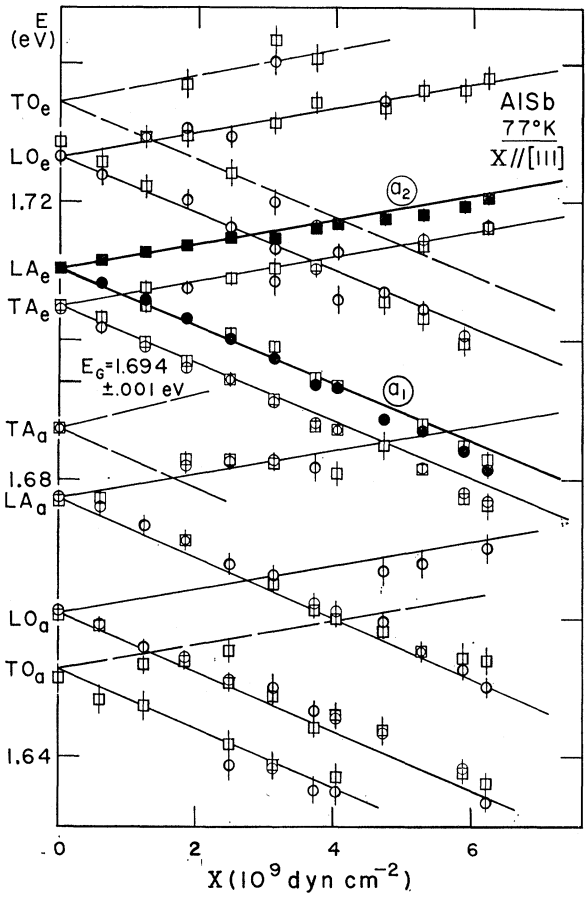

FIG. 5. Stress dependence of the exciton energies as a function of [111] stress for light polarized parallel (circles) and perpendicular (squares) to the stress axis. The solid points show the LA_e exciton thresholds from which the deformation potentials a_i and d have been obtained. The stress-induced splittings of the other excitons were drawn parallel to the LA_e exciton lines in order to fit the experimental points. The TO phonon energy is found to be at (42±3) meV. TA_e excitons were not observed. A value of 1.694±0.001 eV for the indirect gap was obtained from the emission and absorption branches of the spectrum.

[21] E. Erlbach, Phys. Rev. **150**, 767 (1966).

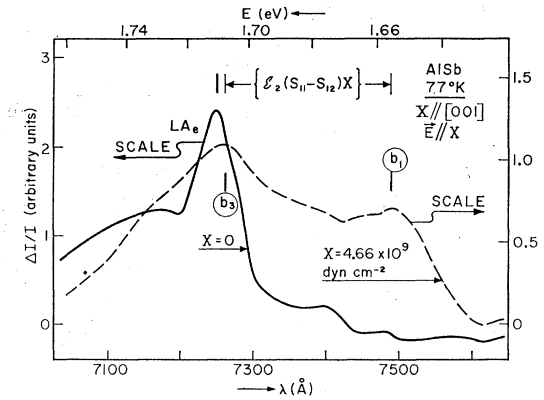

FIG. 6. Derivative transmission spectra for zero stress and for a [001] stress of 4.66×10^9 dyn cm^{-2} for light polarized parallel to the stress axis.

best followed by plotting lines from the zero-stress position parallel to the trajectory of the split LA_e peaks. This figure gives some evidence of the TO-assisted transitions at about 40–45 meV. These transitions were not observed earlier but they were predicted to occur at 41 ± 3 meV.[3] The observed splittings are linear within the experimental accuracy [Eq. (1) predicts a nonlinear shift of 0.8 meV at 6.3×10^9 dyn cm^{-2}, too small to be observed]. From the splitting and shift of the LA_e line we have determined the deformation potentials a_i and d listed in Table II.

Figure 4 shows selection rules and intensities in qualitative agreement with Fig. 3 and Table I. In particular, the a_2 line is very weak for $\mathbf{E}\|X$: it is only allowed with Δ_1 as an intermediate state. A change of intensity of the sign predicted in Table I was observed for the a_1 line. This change is, however, too small for quantitative comparisons.

B. Stress along [001]

For a stress along [001], the splitting of the valence band is the same as that given by Eq. (1), with δE_{111} replaced by $\delta E_{001}=2b(S_{11}-S_{12})X$. The three equivalent [001] conduction minima now split into a singlet [001] and a doublet [010], [100]. This splitting can be represented by the deformation potential $\mathcal{E}_2$,

$$\Delta E_{001}=\tfrac{2}{3}\mathcal{E}_2(S_{11}-S_{12})X,$$
$$\Delta E_{100,010}=-\tfrac{1}{3}\mathcal{E}_2(S_{11}-S_{12})X. \quad (3)$$

The hydrostatic shift of the indirect gap is independent of stress direction and given by Eq. (2). The expected scheme of splitting is shown in Fig. 2.

Each phonon-aided exciton peak thus splits into four under the action of [001] stress. The selection rules for these four LA-phonon-aided transitions are easily obtained under the assumption that Γ_{1c} is the dominant intermediate state. As mentioned earlier, the phonon transitions from the Γ_{1c} band to X_1 are isotropic and hence they introduce a factor of 1 for transitions to the singlet [001] and a factor of 2 for transitions to the doublet [100], [010]. The selection rules for $\Gamma_{15}\rightarrow\Gamma_{1c}$ transitions are the same as for [111] stress. The expected intensities at 2.6×10^9 dyn cm^{-2} ($\alpha_0\ll1$, where $\alpha_0=\delta E_{001}/\Delta_0$) are shown schematically in Fig. 3 and listed in Table I.

Figure 6 shows the LA_e-phonon-assisted exciton peak for zero stress and for a [001] stress $X=4.66\times10^9$ dyn cm^{-2} with $\mathbf{E}\|X$. Because of the selection rules of Table I, the observed splitting corresponds to the singlet-doublet splitting of the conduction band $\mathcal{E}_2(S_{11}-S_{12})X$. The observed intensities are not in agreement with those of Fig. 3, if only peak heights are compared. There are several possible explanations for this discrepancy. For sufficiently close peaks, the overlaps of corresponding signals will distort the shape of the spectrum. Also, external structure (which was observed at 7450 Å only for perpendicular polarized light) made difficult comparison between the spectra for the two different polarizations. However, the b_3 and b_4 lines, which correspond to transitions to the conduction-band doublet, seem to broaden as a function of stress more than b_1 and b_2. If this broadening is considered, the agreement with the calculated intensities is better. This broadening could be due, in part, to the elastic scattering from the conduction band doublet to the large density of states provided by the singlet. Figure 7 shows the stress dependence of the four LA_e peaks for [001] stress. As in the case of [111] stress, the non-

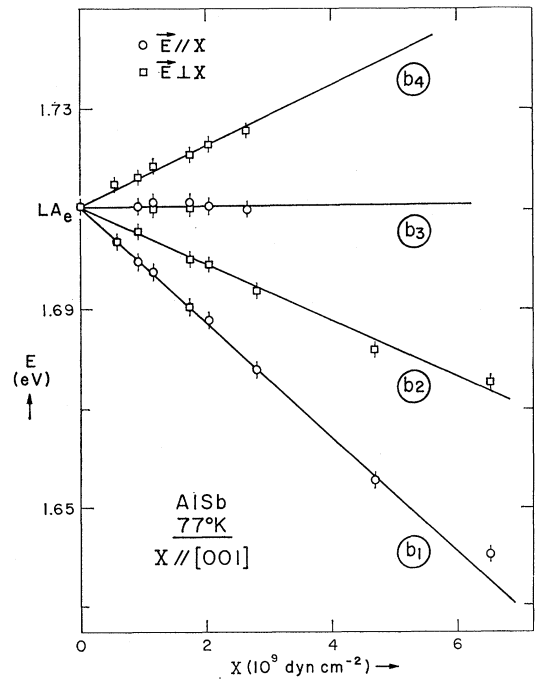

FIG. 7. Stress dependence of the LA_e phonon-assisted exciton for the case of [001] stress. The split lines are labelled according to Fig. 2. The intensities of the $b_4^{\perp}$ and $b_3^{\parallel}$ lines were too small to be observed for stresses above about 3×10^9 dyn cm^{-2}.

linearities predicted by Eq. (1) are too small to be observed. The deformation potentials b, $\mathcal{E}_2$, and a_i obtained from Fig. 7 are listed in Table II. Because of the fourfold splitting for [001] stress, the values of a_i obtained from these measurements are expected to be less accurate than those obtained from [111] stress. Nevertheless, the agreement between both determinations of a_i is quite satisfactory.

C. Stress along [110]

A [110] stress couples both v_1 and v_2 bands to the spin-orbit split band. Hence, v_1 and v_2 should have a nonlinear dependence on stress. The pure shear component of the stress dependence of the energies of the v_1 and v_2 bands is, to second order in X,[18]

$$\begin{aligned}\Delta E_{v_1}&=\tfrac{1}{4}[(\delta E_{001})^2+3(\delta E_{111})^2]^{1/2}\\&\quad+\tfrac{1}{32}[(\delta E_{001})+3(\delta E_{111})]^2/\Delta_0,\\\Delta E_{v_2}&=-\tfrac{1}{4}[(\delta E_{001})^2+3(\delta E_{111})^2]^{1/2}\\&\quad+\tfrac{3}{32}[\delta E_{001}-\delta E_{111}]^2/\Delta_0,\end{aligned}\tag{4}$$

where δE_{001} and δE_{111} have been defined earlier. The measurements for [001] and [111] stress have shown that $\delta E_{001}\approx\delta E_{111}$. Under these conditions, Eq. (4) yields a behavior very similar to that found for [001] and [111] stress. We shall write $\epsilon=(\delta E_{001}-\delta E_{111})/(\delta E_{001}+3\delta E_{111})$. By expanding Eq. (4) in power series of $\epsilon(\epsilon\sim0.002)$ and keeping only first-order terms, we find

$$\begin{aligned}\Delta E_{v_1}&=\tfrac{1}{2}\delta E_{110}+[(\delta E_{110})^2/2\Delta_0],\\\Delta E_{v_2}&=-\tfrac{1}{2}\delta E_{110},\end{aligned}\tag{5}$$

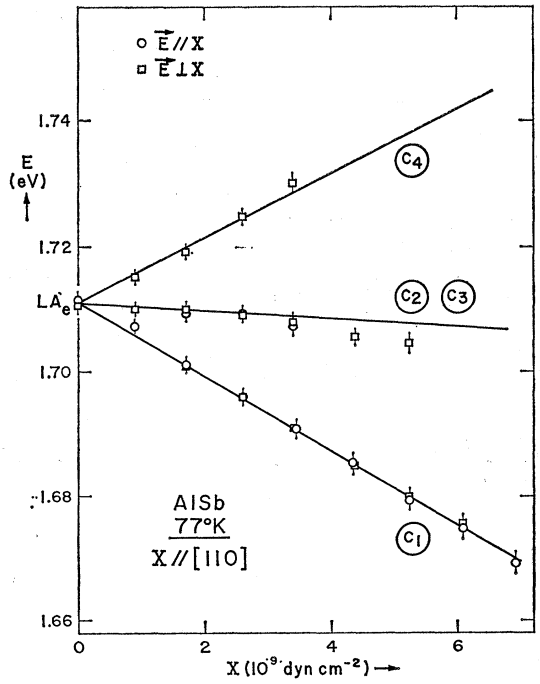

FIG. 8. LA_e phonon-assisted exciton energies as a function of [110] stress.

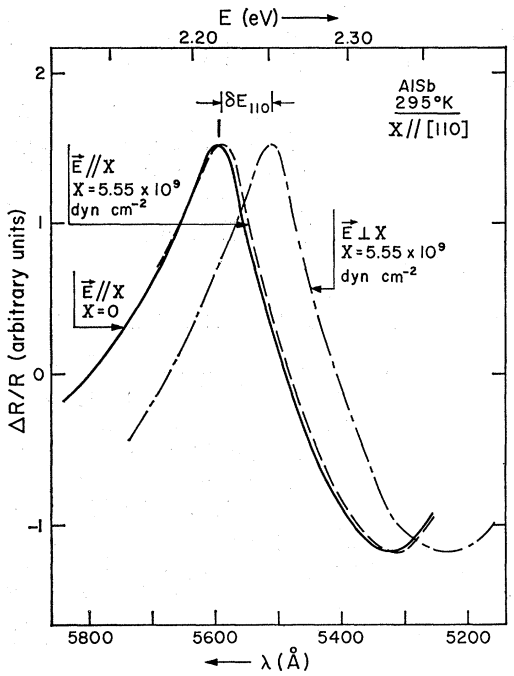

FIG. 9. Electroreflectance spectrum of the E_0 peak ($\Gamma_{15}\rightarrow\Gamma_{1c}$) of AlSb for zero stress and a stress of 5.5×10^9 dyn cm^{-2} along [110] for both polarizations showing the δE_{110} splitting of the $P_{3/2}$ multiplet of the Γ_{15} valence band.

where

$$\delta E_{110}=\tfrac{1}{4}(\delta E_{001}+3\delta E_{111})=\tfrac{1}{4}[2b(S_{11}-S_{12})+d\sqrt{3}S_{44}]X.$$

The X_1 conduction bands also split under the action of a [110] stress: The pattern of splitting is opposite to that obtained for [001] stress (see Fig. 2). The total splitting is half that obtained for the same [001] stress. Instead of Eq. (3), we obtain

$$\begin{aligned}\Delta E_{001}&=-(\mathcal{E}_2/3)(S_{11}-S_{12})X,\\\Delta E_{100,010}&=(\mathcal{E}_2/6)(S_{11}-S_{12})X.\end{aligned}\tag{6}$$

The hydrostatic shift of the indirect gap is the same as that found for [001] and [111] stress.

The selection rules for the transitions with Γ_{1c} as intermediate state can be easily written down for $\epsilon\ll1$. They are similar to those for [001] stress, with δE_{001} replaced by δE_{110}. The expected intensities are represented schematically in Fig. 3 (for $X=2.6\times10^9$ dyn cm^{-2}).

The splitting of the LA_e line alone as a function of [110] stress is shown in Fig. 8. The c_2 and c_3 lines are almost accidentally degenerate. From these data, we can derive $\mathcal{E}_2=+(5.1\pm0.7)$ eV and $a_i=+(2.7\pm1.3)$ eV. Figure 8 also yields δE_{110} and hence the b and d combination

$$\delta E_{110}/X=\tfrac{1}{4}[2b(S_{11}-S_{12})+d\sqrt{3}S_{44}].\tag{7}$$

The value obtained from Fig. 8 for this combination of b and d is shown in Table II to agree with that calculated from the [001] and [111] measurements.

TABLE III. Hydrostatic pressure coefficients (in units of 10^{-6} eV bar^{-1}) of the indirect gaps of Ge, Si, GaP, and AlSb as obtained from uniaxial and hydrostatic stress experiments.

	Ge	Si	GaP	AlSb
Uniaxial	$+3\pm1$[a]	-3.8 ± 0.5[a]	-4.5 ± 1.5[b]	-3.5 ± 0.3[c]
Hydrostatic	$+5$[d]	-1.5[d]	-1[d]	-1.5[d]

[a] I. Balslev, Phys. Rev. **143**, 636 (1966).
[b] I. Balslev, J. Phys. Soc. Japan Suppl. **21**, 101 (1966).
[c] This paper.
[d] Ref. 23.

IV. ELECTROREFLECTANCE AT DIRECT EDGE

Figure 9 shows electroreflectance spectra[7] near 2.2 eV of AlSb without stress and with a [110] stress of 5.55×10^9 dyn cm^{-2}. These measurements were performed at room temperature. The peak in Fig. 9 is believed to correspond to the lowest direct edge ($\Gamma_{15}\rightarrow\Gamma_{1c}$) of this material; it should, therefore, exhibit the δE_{110} splitting of the valence band and the appropriate selection rules. The peak for $\mathbf{E}\|X$ should correspond to $v_1\rightarrow\Gamma_{1c}$ transitions while that for $\mathbf{E}\perp X$ should correspond mainly to $v_2\rightarrow\Gamma_{1c}$ transitions. The value of δE_{110} obtained on the basis of this interpretation agrees with that found from the measurements of the indirect edge (see Table II). Figure 9 shows also a hydrostatic shift for the center of the two split peaks. From this shift in the center of mass we find the hydrostatic deformation potential of the direct edge: $a_d=-5.9\pm1.2$ eV.

V. CONCLUSIONS

We have determined the shear deformation potentials of the Γ_{15} valence band of AlSb and the hydrostatic deformation potentials of its lowest direct and indirect gaps. The pattern of splittings of the indirect edge of this material confirms rather conclusively the [001] symmetry of the corresponding conduction-band minima. An examination of the evolution of the indirect exciton spectrum with stress has enabled us to identify the TO-phonon-aided peak and, thus, to determine the energy of these phonons at X. The splitting of the direct edge and its selection rules confirm its previous assignment to $\Gamma_{15}\rightarrow\Gamma_{1c}$ transitions.[7]

The obtained shear deformation potentials b and d are in line with these found for other III-V compounds (e.g., for GaAs $b=-2.6\pm0.2$ eV, $d=-4.7\pm0.3$ eV).[18,22,23] They correspond to splittings nearly independent of stress direction ($\delta E_{111}\approx\delta E_{001}$). This fact seems to be characteristic of III-V compound since for Ge and Si $\delta E_{111}<\delta E_{001}$ and for II-VI compound $\delta E_{111}>\delta E_{001}$.[22]

The hydrostatic deformation potentials of the indirect gap determined from measurements for three stress directions (Table II) agree within the experimental error. The best accuracy for a_i [$+(2.2\pm0.2)$ eV], has been obtained for $X\|[111]$. This deformation potential can be easily converted into the hydrostatic pressure coefficient $(\partial E/\partial P)_i$,

$$\left(\frac{\partial E}{\partial P}\right)_i=-3(S_{11}+2S_{12})a_i=-(3.5\pm0.3)\times10^{-12}\text{ eV dyn}^{-1}\text{ cm}^2$$
$$=-(3.5\pm0.3)\times10^{-6}\text{ eV bar}^{-1}.$$

We notice that this coefficient is considerably larger than that quoted in the literature (-1.5×10^{-6} eV bar^{-1}),[23] obtained from optical measurements under hydrostatic stress at room temperature. Similar discrepancies between low-temperature uniaxial stress and room-temperature hydrostatic stress data exist for other indirect gap materials, such as Si, Ge, and GaP (see Table III). While we do not know the source of this discrepancy, one might speculate that the optical measurements of the indirect gap at room temperature are based on a detailed analysis of the changes of the line shape with stress[24] and hence are not very reliable. However, results in agreement with the shift of the indirect edge with hydrostatic pressure have been obtained from radiative recombination at 80°K [25] and from electrical measurements under hydrostatic pressure.[24] We are thus led to conclude that the discrepancy is related to the uniaxial nature of the applied stress in a manner not understood by us.

The hydrostatic pressure coefficient obtained for the $\Gamma_{15}\rightarrow\Gamma_{1c}$ direct gap is $(\partial E/\partial P)_d=+(10\pm2)\times10^{-6}$ eV bar^{-1}. This coefficient has not been determined from hydrostatic pressure measurements. However, it is approximately equal to that found for most other materials of this family[25] [$(\partial E/\partial P)_d\approx+11\times10^{-6}$ eV bar^{-1}].

[22] A. Gavini and M. Cardona, Phys. Rev. (to be published).

[23] R. N. Bharagava and M. I. Nathan, Phys. Rev. **161**, 695 (1967).

[24] W. Paul and P. M. Warschauer, J. Phys. Chem. Solids **5**, 89 (1958); **5**, 102 (1958).

[25] R. Zallen and W. Paul, Phys. Rev. **134**, A1628 (1964); **155**, 703 (1967).